

Oral delivery of gambogenic acid by functional polydopamine nanoparticles for targeted tumor therapy

Beilei Wang^{a,1}, Tengteng Yuan^{a,1}, Liqiong Zha^a, Yuanxu Liu^a, Weidong Chen^a, Caiyun Zhang^{a,*}, Youmei Bao^{b,*}, Qiannian Dong^{a,*}

^aSchool of Pharmacy, Anhui University of Chinese Medicine, Anhui Academy of Chinese Medicine, Hefei 230012, Anhui, China

^bSchool of Pharmaceutical Sciences, Southern Medical University, Guangzhou 510515, PR China

¹These authors contributed to the work equally and should be regarded as co-first authors.

*Corresponding author. School of Pharmacy, Anhui University of Chinese Medicine, Anhui Academy of Chinese Medicine, Hefei 230012, Anhui, China

*Corresponding author. School of Pharmaceutical Sciences, Southern Medical University, Guangzhou 510515, PR China

E-mail: cyzhang6@ustc.edu.cn (C.Y. Zhang); yumei.bao@hotmail.com (Y.M. Bao); dongqn2005@126.com (Q.N. Dong)

NMR analysis and purity of Gambogenic acid (GNA)

¹³C NMR spectrum of GNA was recorded using a Bruker Advance 400 MHz spectrometer with deuterated methanol (MeOD) as the solvent.

Purity of GNA was determined by HPLC (Agilent, Waldbronn, Germany) as Reference ¹. The column (ZORBAX Eclipse XDB-C8 column, 5 μm, φ4.6mm×150mm, Agilent, U.S.A.) was eluted with a binary mixture of acetonitrile and 0.20% acetic acid solution (volume ratio 85:15) at a flow rate of 1.0 ml/min. Elution was monitored at 360nm on a diode array detector. The injection volume was 10 μL (5 μg·mL⁻¹ gambogenic acid) and the column temperature was maintained at 25°C.

Fourier transform infrared spectra and differential scanning calorimetry

Fourier transform infrared spectra (FTIR) was used to confirm the chemical reaction between PDA and FA. The samples were mixed with KBr powder. The infrared spectrometer of 400-4000 cm⁻¹ wave number was utilized to scan the mixture by a Bruker Vector 22 FTIR spectrometer.

The thermograms of GNA and lyophilized GNA@PDA-FA SA NPs were investigated by means of differential scanning calorimetry (DSC) (Q200 F3 NETZSCH, Selb, Germany). About 5 mg of sample was placed into an aluminium pan and sealed in the airproof conditions. The thermal behavior was performed from 30 to 200 °C at a scanning rate of 5 °C/min ².

The water solubility of GNA and GNA@PDA-FA SA NPs

Excess raw GNA was added to ultrapure water and centrifuged (12000 rpm for 10 min) after fully dissolving, then, the supernatant was injected in HPLC to get the water solubility of GNA.

***In vitro* drug release of GNA@PDA-FA SA NPs in simulated gastrointestinal fluid**

In vitro drug release of GNA@PDA-FA NPs, GNA@PDA SA NPs and raw GNA were conducted with dialysis bags diffusion in release medium of simulated gastrointestinal fluid without enzyme. In detail, 1.75 mL GNA solution (0.7 mg GNA dissolved into 1.75 mL of ethanol), 1.75 mL GNA@PDA NPs solution and 1.75 mL GNA@PDA-FA SA NPs solution (equivalent to 0.7 mg of GNA) were placed into three per-swelled dialysis bags (≤ 12 kDa, China). The bags were separately immersed in 100

mL simulated gastric fluid for 2h and then in simulated gastrointestinal fluid for another 7h with stirring at 100 rpm and 37 ± 0.5 °C, respectively. At predetermined intervals (0.5, 1, 2, 4, 6, 9, 12, 24, 36, 48, 72 h), 500 μ L release aliquots medium was taken out for analysis, at the same time 500 μ L fresh release medium was added to the outer solution.

Results

Detailed data on NMR analysis and purity of Gambogic acid (GNA)

Figure S1 showed the ^{13}C NMR spectrum of GNA with the characteristic chemical shift at δ 16.1, 17.6, 17.9, 20.6, 21.0, 22.0, 25.2, 25.6, (2C), 26.3, 28.9, 29.5, 29.8, 39.7, 46.9, 48.9, 83.7, 84.0, 90.4, 100.6, 106.4, 107.4, 121.4, 122.0, 123.8, 128.1, 131.7, 133.6 (2C), 135.0, 138.1, 138.9, 155.9, 160.3, 163.5, 172.1, 179.1, 203.5, which were consistent with the literature data ³.

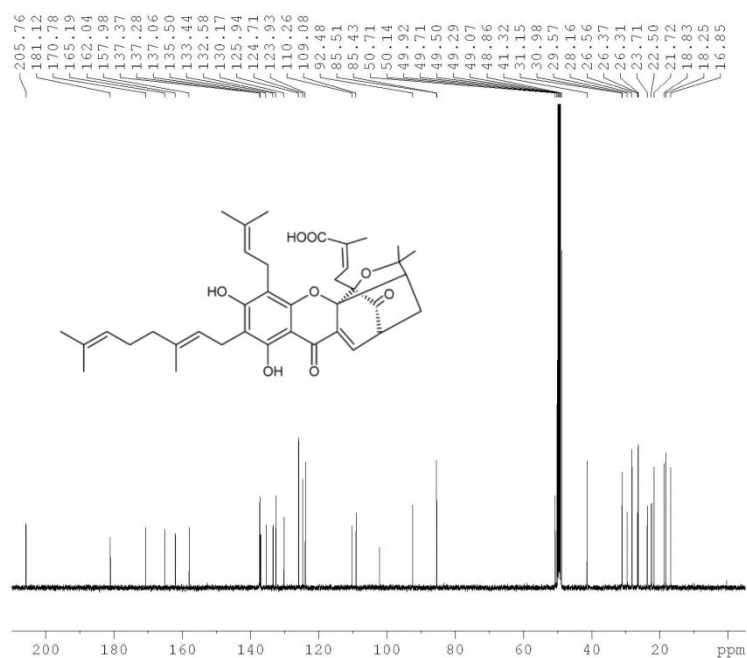


Fig S1. ^{13}C NMR spectrum of GNA

As shown in Fig S2, the purity of GNA was 98% determined by HPLC.

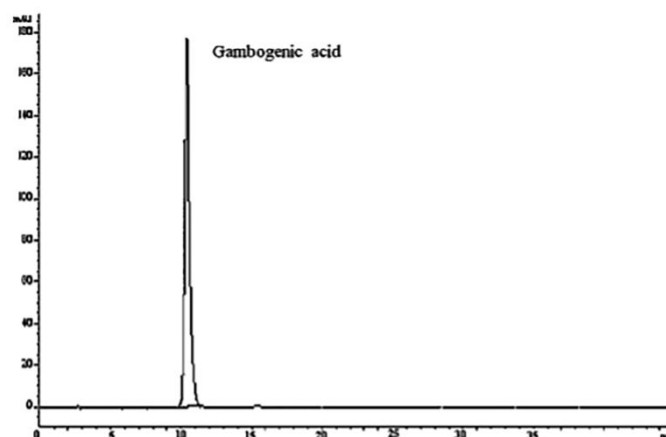


Fig S2. HPLC-UV Chromatograms of GNA

Fourier transform infrared spectra and differential scanning calorimetry of GNA@PDA-FA SA NPs

As shown in Fig S3(a), the FTIR of GNA exhibits strong absorption bands at 1450 cm^{-1} and 1630 cm^{-1} which are attributed to C-H vibration of benzene ring and C=O vibration of amide, respectively. The characteristic band at 2970 cm^{-1} was attributed to the carboxyl stretching vibration of GNA. FTIR in Fig S3(a) provided the information about the chemical composition of GNA@PDA NPs and GNA@PDA-FA NPs. The broad and strong absorption at $3400\text{--}3300\text{ cm}^{-1}$ was assigned to the stretching vibrations of N-H and O-H. The absorption peak at 1651 cm^{-1} originated from C=O of amide in stretching mode, and peaks at 1500 cm^{-1} , 1470 cm^{-1} and 1460 cm^{-1} were attributed to C-H vibration of benzene ring⁴. The peak at 2943 cm^{-1} was assigned to C-H vibration of alkane and became stronger after reaction with FA⁵. Compared to the FTIR of GNA, GNA@PDA NPs and GNA@PDA-FA NPs exhibited new absorption bands at 1020 cm^{-1} and 1090 cm^{-1} , which are attributed to the stretching vibrations of C-N groups. Meanwhile, both absorption bands at 1020 cm^{-1} and 1090 cm^{-1} were significantly increased after FA function in GNA@PDA-FA NPs. These changes indicated that chemical reaction between FA and PDA may occur through the formation of amide.

DSC is a reliable method to provide insight into the possible interactions between PDA and FA. As shown in Fig. S3(b), a clear single melting endothermic peak of raw GNA was observed at $108\text{ }^{\circ}\text{C}$, which was in agreement with the reported data⁶. After

GNA being captured in the PDA nanoparticles, the melting peak of GNA slightly shifted and turned broader in comparison with raw GNA. Moreover, a new endothermic peak appeared at 145 °C after the GNA@PDA-FA NPs formation, which indicated success conjugation of FA to the PDA core.

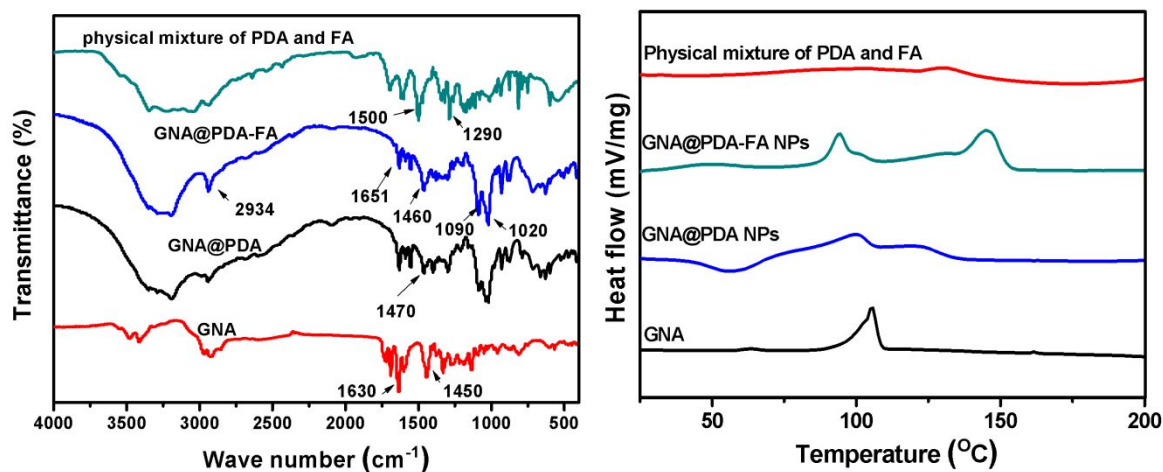


Fig S3. (a) FTIR spectra of physical mixture of PDA and FA, GNA@PDA-FA NPs, GNA@PDA NPs and raw GNA. (b) DSC of GNA, GNA@PDA NPs, GNA@PDA-FA NPs and physical mixture of PDA and FA, respectively.

The water solubility of GNA and GNA@PDA-FA SA NPs

Table S1 The water solubility of GNA and GNA@PDA-FA SA NPs ($n = 3$)

| Samples | Pure GNA | GNA@PDA-FA SA NPs |
|--------------------------|-------------|-------------------|
| Water solubility (µg/mL) | 0.27 ± 0.05 | 418.33 ± 5.51 |

In this work, 0.4 mg GNA was loaded in 1 mL GNA@PDA-FA SA NPs solution (containing 0.4 mg GMA, 0.2 mg PDA, 0.2 mg FA and 0.4 mg SA) under optimal conditions, while the water solubility of pure GNA is about 0.27 µg/mL (Table S1). It can be seen that GNA@PDA-FA SA NPs greatly improved the water solubility of GNA.

In vitro drug release of GNA@PDA-FA SA NPs in simulated gastrointestinal fluid

To investigate the stability and in vitro drug release of this oral formulation in gastrointestinal environment, the release of GNA@PDA-FA SA NPs were firstly carried out in simulated gastric fluid for 2h. The cumulative release percentages of

GNA@PDA-FA SA NPs at 1 h and 2 h were 1.65 % and 4.50 %, respectively. Then, we performed in vitro drug release of GNA@PDA-FA SA NPs in simulated intestinal fluid. As shown in Fig S4, accumulatively, up to 8.58% and 6.36% of GNA was released from GNA@PDA-FA NPs and GNA@PDA-FA SA NPs at 8h, respectively. The above results showed that GNA@PDA-FA NPs released a small amount of drug in simulated gastrointestinal fluid, indicating that NPs designed in this study can pass steadily through the gastrointestinal environment after oral administration.

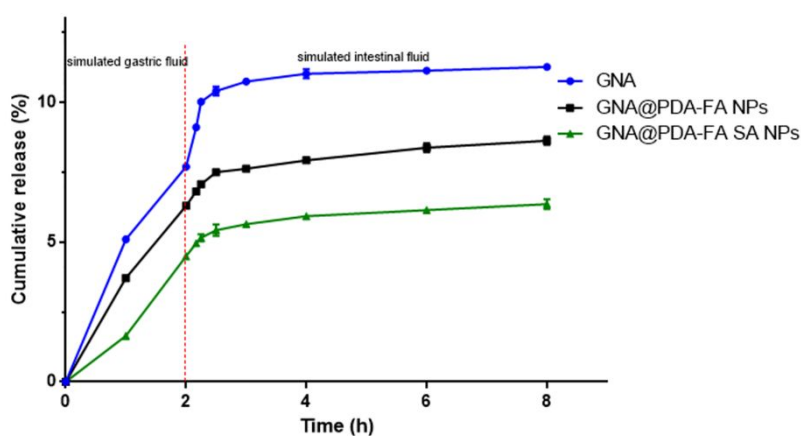


Fig S4. Release profiles of raw GNA, GNA@PDA-FA NPs and GNA@PDA-FA SA NPs in simulated intestinal fluid at 37 ± 0.5 °C (n = 3).

References

1. Li, Q.; Cheng, H.; Zhu, G.; Yang, L.; Zhou, A.; Wang, X.; Fang, N.; Xia, L.; Su, J.; Wang, M.; Peng, D.; Xu, Q. Gambogic acid inhibits proliferation of A549 cells through apoptosis-inducing and cell cycle arresting. *Biological & pharmaceutical bulletin* **2010**, *33*, (3), 415-20.
2. Abdelraof, M.; Hasanin, M.; El-Saied, H. Ecofriendly green conversion of potato peel wastes to high productivity bacterial cellulose. *Carbohydrate polymers* **2019**, *211*, 75-83.
3. Asano, J.; Chiba, K.; Tada, M.; Yoshii, T. Cytotoxic xanthenes from *Garcinia hanburyi*. *Phytochemistry* **1996**, *41*, (3), 815-20.
4. Bi, D.; Zhao, L.; Yu, R.; Li, H.; Guo, Y.; Wang, X.; Han, M. Surface modification of doxorubicin-loaded nanoparticles based on polydopamine with pH-sensitive property for tumor targeting therapy. *Drug delivery* **2018**, *25*, (1), 564-575.
5. Yu, X.; Fan, H.; Wang, L.; Jin, Z. Formation of polydopamine nanofibers with the aid of folic acid. *Angewandte Chemie (International ed. in English)* **2014**, *53*, (46), 12600-4.
6. Liu, S.; Liu, J.; Cong, J.; Tong, L.; Zhang, Y.; Li, X.; Hou, J. Preparation of Neogambogic Acid Nanoliposomes and its Pharmacokinetics in Rats. *Journal of the College of Physicians and Surgeons--Pakistan : JCPSP* **2018**, *28*, (12), 937-940.